

Supplementary Information

Ambient-Dried Highly Flexible Copolymer Aerogels and their Nanocomposites with Polypyrrole for Thermal Insulation, Separation, and Pressure Sensing

Guoqing Zu,^{1,} Kazuyoshi Kanamori,^{2,*} Ayaka Maeno,³ Hironori Kaji,³ Kazuki Nakanishi², Jun Shen⁴*

¹School of Materials Science and Engineering, Tongji University, Shanghai 201804, P. R. China

²Department of Chemistry, Graduate School of Science, Kyoto University, Kitashirakawa, Sakyo-ku, Kyoto 606-8502, Japan

³Institute for Chemical Research, Kyoto University Gokasho, Uji, Kyoto 611-0011, Japan

⁴Shanghai Key Laboratory of Special Artificial Microstructure Materials and Technology, Pohl Institute of Solid State Physics, Tongji University, Shanghai 200092, P. R. China

*Corresponding authors:

E-mail: guoqingzu@tongji.edu.cn (G. Zu),

kanamori@kuchem.kyoto-u.ac.jp (K. Kanamori)

This PDF file includes:

Captions for Movies S1 to S4

Figures S1 to S8

Other Supplementary Materials for this manuscript include the following:

Movies S1 to S4

Movie list:

Movie S1. High compression flexibility of VT21P shown by hand compression.

Movie S2. High bending flexibility of VT51 shown by hand bending.

Movie S3. Efficient separation of *n*-octane and water with VT21.

Movie S4. Strain-sensitive conductivity of VT21P.

Figures:

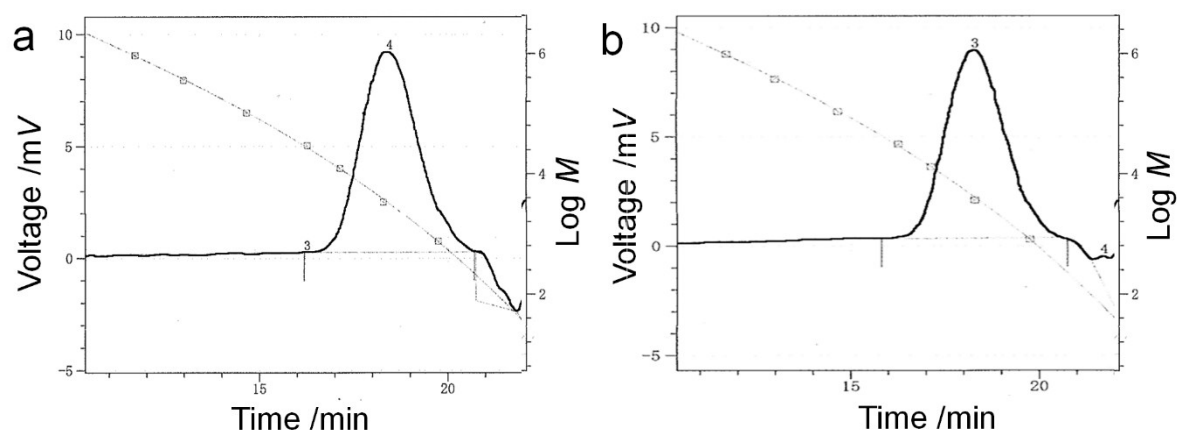


Figure S1. The GPC data of (a) VT21 and (b) VT51. The measured number-average molecular weight (M_n), M_w , and M_w/M_n of VT21 were 2340, 4149, and 1.77, respectively, while the M_n , M_w , and M_w/M_n of VT51 were 2770, 4995, and 1.80, respectively.

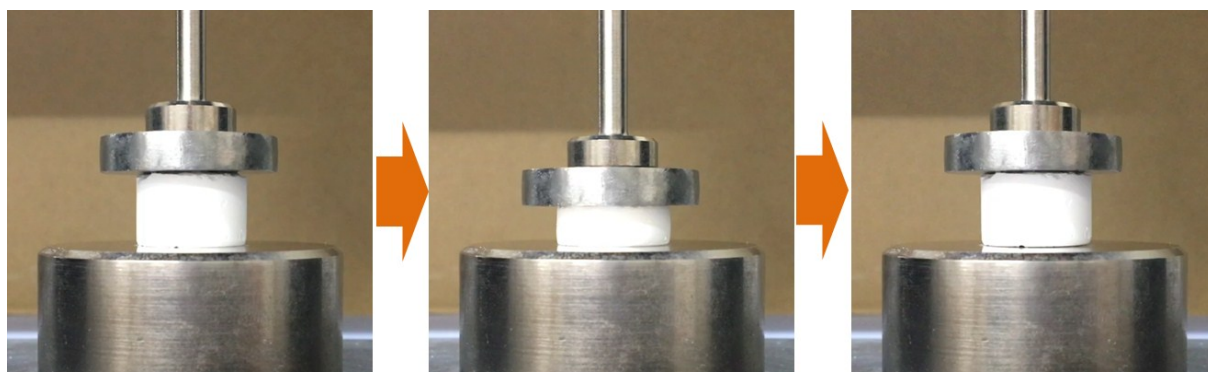


Figure S2. Photographs of a uniaxial compression–decompression test on VT11.

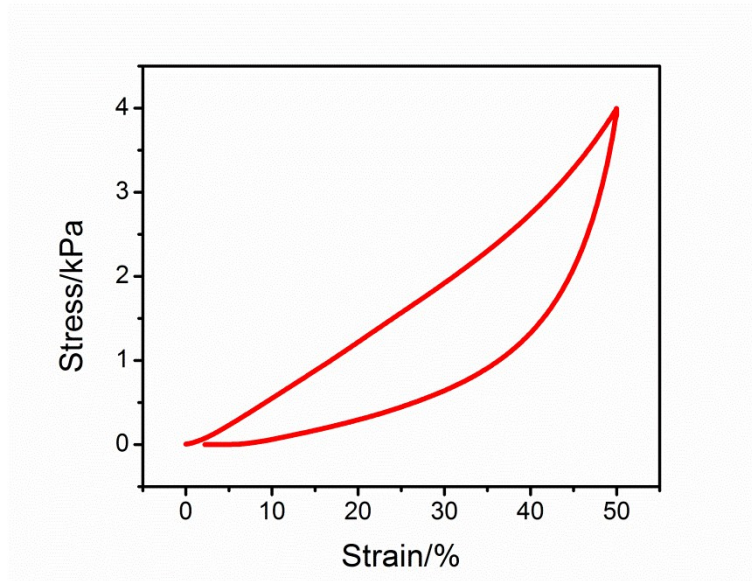


Figure S3. Stress–strain curves of a uniaxial compression–decompression test on VT11.

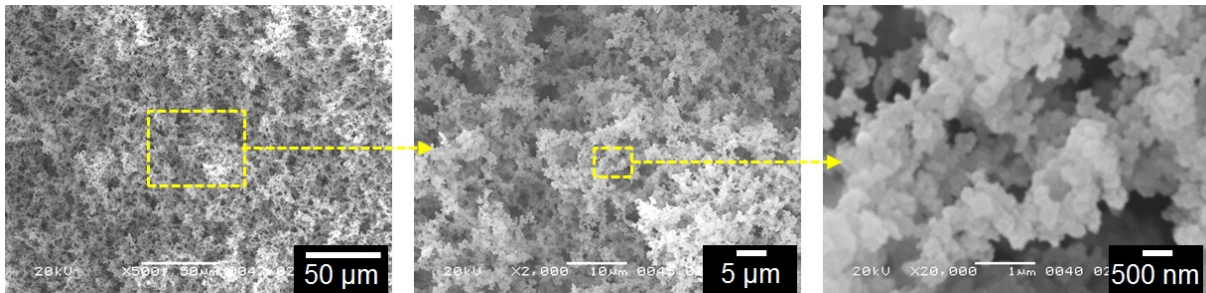


Figure S4. SEM images of VT21 after compression–decompression with 50% strain for 100 cycles.

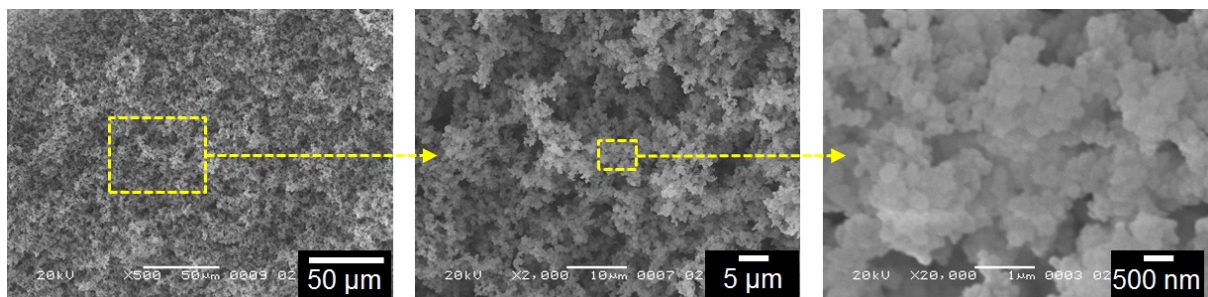


Figure S5. SEM images of VT21P after compression–decompression with 50% strain for 100 cycles.



Figure S6. Photographs of a three-point bending test on VT21.

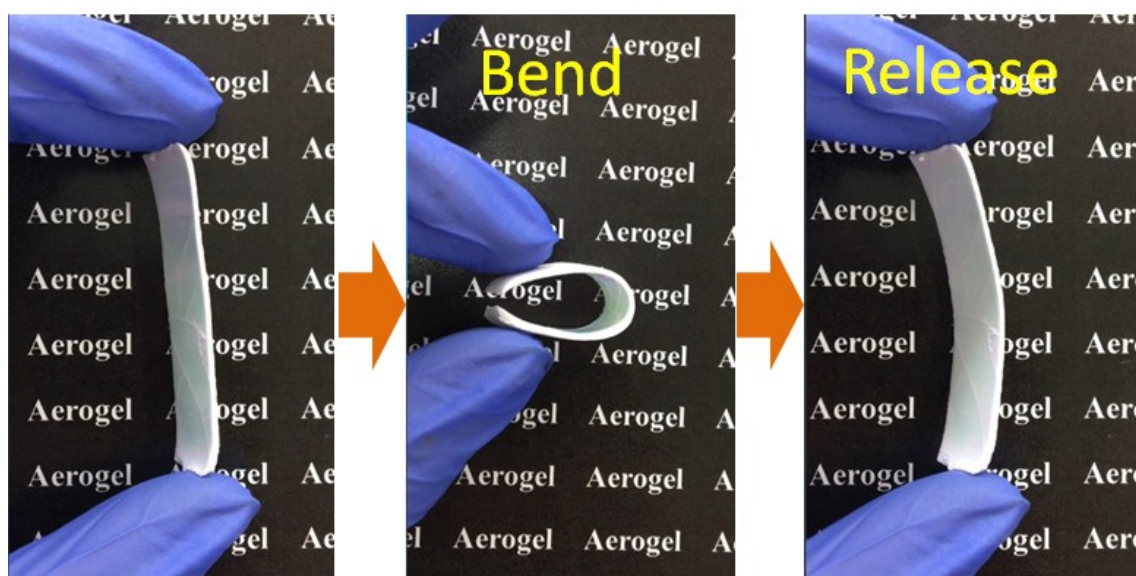


Figure S7. Photographs of a hand bending test on VT21

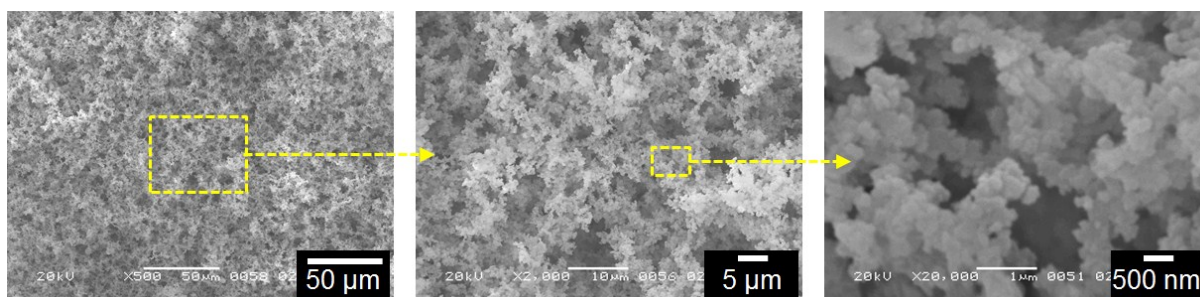


Figure S8. SEM images of VT21 after absorption for *n*-octane and drying for 10 cycles. Its morphology remains unchanged after 10 cycles.